https://doi.org/10.5194/ar-2025-16
Preprint. Discussion started: 2 June 2025
© Author(s) 2025. CC BY 4.0 License.

AEROSOL Research Discussions

Long-term PM trends in southern Finland from three different measurement techniques

Ilona Ylivinkka[1,2], Helmi-Marja Keskinen[1], Lauri R. Ahonen[1,2], Liine Heikkinen[1,3,4], Pasi P. Aalto[1], Tuomo Nieminen[1,5], Katrianne Lehtipalo[1,6], Juho Aalto[2,7], Janne Levula[1], Jutta Kesti[1,6], Ekaterina Ezhova[1], Markku Kulmala[1], and Tuukka Petäjä[1]

[1]Institute for Atmospheric and Earth System Research (INAR) / Physics, Faculty of Science, University of Helsinki, Helsinki, 00014, Finland
[2]Station for Measuring Ecosystem - Atmosphere Relations II (SMEAR II), University of Helsinki, Korkeakoski, 35500, Finland
[3]Department of Environmental Science, Stockholm University, Sweden
[4]Bolin Centre for Climate Research, Stockholm University, Sweden
[5]Department of Physics, Faculty of Science, University of Helsinki, Finland
[6]Finnish Meteorological Institute, 00560 Helsinki, Finland
[7]Institute for Atmospheric and Earth System Research (INAR) / Forest Sciences, Faculty of Agriculture and Forestry, University of Helsinki, Helsinki, 00014, Finland

Correspondence to: Ilona Ylivinkka (ilona.ylivinkka@helsinki.fi)

Abstract. Different particulate matter (PM) mass concentration measurements and their long-term trends were compared at the Station for Measuring Ecosystem-Atmosphere Relations (SMEAR II, Hyytiälä, Finland). We compare three independent methods: 1) gravimetric method with a cascade impactor, 2) Synchronized Hybrid Ambient Real-time Particulate Monitor (SHARP), and 3) calculated PM concentration from combined Differential Mobility Particle Sizer (DMPS) and Aerosol Particle Sizer (APS) particle number size distribution data. In all size classes (PM_1, $PM_{2.5}$ and PM_{10}), the different methods show a good correlation (Pearson's correlation coefficient approximately 0.8). The mass concentrations in all PM classes were the highest in summer and the lowest in autumn and winter. While all seasons and size classes showed declining trends for PM concentrations (from -0.012 to -0.064 μg m^{-3} y^{-1}) between 2005 and 2020, the decline was smallest in summer, which follows the trends observed also in SO_2 and NO_x concentrations. These results underline both the summertime dominance of biogenic sources for the aerosol mass concentration in the rural boreal forest environment and the reduction of anthropogenic pollution due to the EU level restrictions for improved air quality.

https://doi.org/10.5194/ar-2025-16
Preprint. Discussion started: 2 June 2025
© Author(s) 2025. CC BY 4.0 License.

1 Introduction

Particulate matter (PM) concentrations are monitored worldwide, because they are connected to health effects, such as asthma and cardiovascular diseases, and premature deaths (Pope et al., 2003; Shiraiwa et al., 2017; WHO, 2021). The increased knowledge regarding the relationship between air pollution and mortality have resulted in air pollution regulations, which additionally aim to decrease inequality related to air pollution exposure (Wang et al., 2017; WHO, 2021). Besides the adverse health effects, aerosol particles can also scatter or absorb radiation and participate in cloud formation and processing, thus affecting the Earth's climate (IPCC, 2021). While the overall effect of aerosol particles on climate is considered to be cooling, large uncertainty is related to aerosol particles and especially aerosol-cloud-radiation interactions (IPCC, 2021).

The PM measurements are divided into size classes based on the aerodynamic diameter of the particles: PM_1, $PM_{2.5}$, and PM_{10} with upper maximum diameters of particles 1 µm, 2.5 µm, and 10 µm, respectively. The PM mass concentrations in the size fractions are the total mass of particles below these limiting sizes. The size of atmospheric aerosol particles is perhaps their most critical parameter, both in terms of their climate (e.g., Pöschl, 2005; Dusek et al., 2006) and health effects (Schraufnagel, 2020). In principle, the smaller the particles are, the deeper they can penetrate in the human respiratory system and can thus end up also in other organs beside the lungs (Pope et al., 2003; Maynard & Kuempel, 2005). To address this, the new air quality directive of the European Union (2024/2881) includes total concentration and size distribution measurements of ultrafine particles (defined as particles between 10 to 100 nm in diameter) as well as black carbon (BC) as mandatory measurement parameters at air quality supersites, as suggested e.g. by Kuula et al. (2021). The smallest particles have only a minor contribution to the aerosol mass concentration, but they dominate the particle number concentration. In the climate perspective, the most relevant particles have a diameter larger than about 50–100 nm, since they can act as cloud condensation nuclei and scatter or absorb radiation (IPCC, 2021).

The sources of aerosol particles are variant, including both local and long-range transported emissions, since the lifetime of particles is about one week (Seinfeld and Pandis, 2006; Manavi et al., 2025). Primary aerosol particles consist mostly of particles from traffic and industry (e.g., BC), or from natural sources (e.g., volcanic ash, sea-spray, dust, and pollen), and they

https://doi.org/10.5194/ar-2025-16
Preprint. Discussion started: 2 June 2025
© Author(s) 2025. CC BY 4.0 License.

contribute to all PM classes. Secondary aerosol particles are formed in the atmosphere from gas-phase precursor vapors (e.g. Kulmala et al., 2013), including, for example, different oxidized organic compounds, sulfuric acid, ammonia, and amines (e.g. Olenius et al., 2018). These eventually grow to larges size ranges contributing significantly to the accumulation mode and thereby to PM_1.

Organic aerosol (OA) is a major PM_1 component at SMEAR II (Heikkinen et al., 2020) and globally (e.g. Jimenez et al., 2009). Biogenic or anthropogenic emissions of volatile organic compounds (VOCs) are major OA sources. They undergo oxidation in the atmosphere yielding oxygenated products with lower volatilities than the parent VOC. These oxidation products can grow pre-existing particles e.g., via condensation (e.g. Riipinen et al., 2012), thereby increasing the PM loadings. In the boreal coniferous forest, the VOCs consist largely of monoterpenes, emitted by the surrounding vegetation (Rinne et al., 2005). The emission rates of monoterpenes from the forest are boosted by warm temperatures (Guenther et al., 1993). The same is observed in the OA mass concentrations (Heikkinen et al., 2021; Yli-Juuti et al., 2021). On average, OA is the most abundant aerosol chemical species at SMEAR II (Heikkinen et al., 2020).

Sulfate, another key PM_1 component at SMEAR II and globally, is formed, e.g., upon oxidation from sulfur dioxide (SO_2), mostly emitted by industry (Seinfeld and Pandis, 2006). This may take place either in the gas phase (e.g. SO_2 oxidation by OH) or in the atmospheric aqueous phase, such as in cloud water (e.g. Seinfeld and Pandis, 2006). Sulfate aerosol formation, resulting from cloud processing, has been observed at SMEAR II (Isokääntä et al., 2022).

Nitrate aerosol mass concentrations, mostly prevalent in agricultural or urban environments are therefore less abundant at SMEAR II (Makkonen et al., 2014). The concentration depends on, e.g., the availability of nitric acid (HNO_3), which is an oxidation product of nitrous oxides (NO_x), and gas phase ammonia (NH_3) as well as properties of pre-existing particles (pH and liquid water content) and air temperature (Nenes et al., 2020).

The first EU level legislations concerning air quality entered into force in 2005. Nowadays, the legislation covers basic air pollutants: PM (PM_{10} and $PM_{2.5}$), trace gases (SO_2, NO_2, O_3, CO, benzene, and polyaromatic hydrocarbons) as well as heavy metals (Pb, As, Ni, and Cd). Legislation on PM concerned originally only PM_{10} concentration: the daily 24 h average was targeted to <50 µg m^{-3}, but could be exceeded 35 times per year, and yearly averaged PM_{10}

https://doi.org/10.5194/ar-2025-16
Preprint. Discussion started: 2 June 2025
© Author(s) 2025. CC BY 4.0 License.

value was limited to 40 µg m^{-3}. In 2010, yearly average $PM_{2.5}$ was first targeted to 25 µg m^{-3} and in 2015, it became a limiting value. In 2020, the limit value was tightened to 20 µg m^{-3}. Legislation concerning SO_2, a precursor for sulfuric acid, is from 2005: hourly averaged SO_2 value was limited to 350 µg m^{-3} and 24 h average to 125 µg m^{-3}. NO_2, which is formed in combustion processes, was also regulated: the limit hourly average value was set to 200 µg m^{-3} and yearly average to 40 µg m^{-3} in 2010. The EU level directives can be found in https://environment.ec.europa.eu/topics/air/air-quality/eu-air-quality-standards_en (Accessed: 25 Apr 2025).

The Ambient Air Quality Directive was revised in the end of 2024, forcing further reductions for targets values of many pollutants, including PM_{10}, $PM_{2.5}$, O_3, SO_2, CO, and benzene. Additionally, the new air quality directive introduces advanced measurement parameters, such as aerosol number concentration, aerosol size distribution, BC, and oxidative potential. Air quality supersite concept is implemented as well (Kuula et al., 2021). In order to compare the health impacts of the ultrafine particles and $PM_{2.5}$, the observations are concentrated in urban and rural supersites. The number of the required sites depend on the population and land area of the EU member state. In addition, the EU Commission mandates measurements of ultrafine and BC concentrations in the vicinity of air pollution hotspots.

Techniques for measuring aerosol mass concentrations have improved remarkably during the last decades (Van Dingenen et al., 2004; Occhipinti & Oluwasanya, 2017; Shukla & Aggarwal, 2022). Most of the PM measurements have traditionally been done by an offline gravimetric analyses where particle size classes are separated, e.g., by impactor (Laakso et al., 2003) or special high-volume samplers (Barmpadimos et al., 2011). The offline methods are quite laborious as their sampling time is up to few days and weighing is done manually. Thus, PM concentrations are nowadays more commonly measured with on-line techniques, such as tapered element oscillating microbalance (TEOM) with the Continuous Ambient Particulate Monitor (Laakso et al., 2008) and Synchronized Hybrid Ambient Real-time Particulate monitor (SHARP) (Chen et al., 2018). Besides the direct mass measurements, the particle mass can be calculated from the particle number size distribution with assumptions regarding particles' shape and density (Neusüß et al., 2000).

The aim of this work is threefold. First, we compare the PM concentrations obtained from gravimetric impactor, on-line mass analyzer SHARP and from the particle number size

https://doi.org/10.5194/ar-2025-16
Preprint. Discussion started: 2 June 2025
© Author(s) 2025. CC BY 4.0 License.

distribution to explore their applicability for continuous PM measurements. Second, we report for the first time long-term (2005–2020) measurements of PM_{10}, $PM_{2.5}$ and PM_1 at SMEAR II, Finland, and explore the overall concentration levels as well as selected specific episodes. Third, we estimate the trends of the PM concentrations separately for each season and the impact of the EU legislation on the PM trends. Quality controlled data on aerosol particle mass concentration in a boreal background station enable us to explore the role of local, regional and global phenomena controlling the aerosol mass concentration in the region. This work continues the analysis presented in Keskinen et al. (2020) with updated datasets and revised analysis methods.

2 Methods

2.1 Measurement station

The measurements were performed at SMEAR II located in Hyytiälä in southern Finland (61°51'N, 24°17'E; 181 m a.s.l.; Fig. 1a). Hyytiälä is a rural background measurement site with low local anthropogenic emissions (Hari and Kulmala, 2005). A photo of the homogeneous 60-year-old Scots pine stand surrounding SMEAR II is presented in Fig. 1c. The nearest cities are Tampere (50 km southwest; 249 000 inhabitants) and Jyväskylä (90 km northeast; 146 000 inhabitants).

The station is equipped with instruments for continuous and comprehensive measurements of interactions between the forest ecosystem and atmosphere (Hari and Kulmala et al., 2005). SMEAR II is part of the European Aerosols, Clouds, and Trace gases Research Infrastructure (ACTRIS; Laj et al. 2024; https://www.actris.eu/, accessed 08 Nov 2024). The presented measurements are conducted inside the canopy with total suspended particulates (TSP) or PM_{10} design inlets for the different aerosol measurements on the roof of the aerosol hut (Fig. 1b). Winter at SMEAR II is defined to be from December to February (DJF), spring is from March to May (MAM), summer from June to August (JJA) and autumn from September to November (SON). Note that winter has January and February data from the following year. Due to the data availability, measurements start from spring 2005 and in the end of the measurement period winter includes only December 2020.

https://doi.org/10.5194/ar-2025-16
Preprint. Discussion started: 2 June 2025
© Author(s) 2025. CC BY 4.0 License.

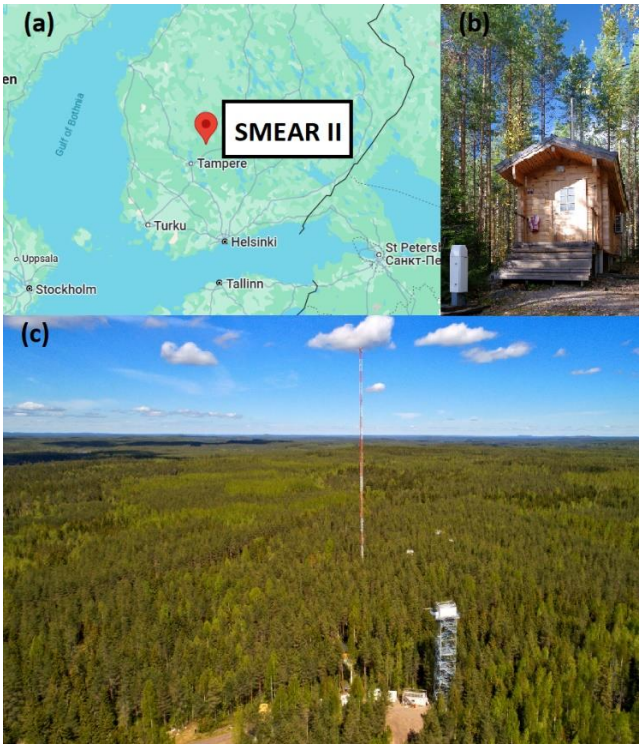

Figure 1: (a) The location of SMEAR II (© OpenStreetMap contributors 2020. Distributed under a Creative Commons BY-SA License), (b) hut for aerosol instrumentation, and (c) a photo of the surrounding region around SMEAR II.

2.2 Weighing-based mass measurements with cascade impactor

PM measurements with gravimetric cascade impactor started in late 1990s at SMEAR II. The impactor has an unheated TSP inlet with stainless-steel tube, placed at 5 m height above the ground. The cascade impactor has three stages with impactor cut points at 10 µm (PM_{10}), 2.5 µm ($PM_{2.5}$) and 1 µm (PM_1) (Dekati PM10 impactor) (Berner and Luerzer, 1980). The sample air flow rate during collection is 30 lpm. Collection substrates are 25 mm polycarbonate membranes (Nuclepore 800 203) without holes. At the last stage there is a 47 mm Teflon filter with 2 µm pore size (R2P J047) from Pall Corporation. To prevent the bouncing back of the particles from the collection substrates, the membranes are greased with Apiezon L vacuum grease diluted in toluene. The collected impactor samples are weighted every two or three days to get the mass distribution. The samples are stored in a freezer for occasional further analyses.

https://doi.org/10.5194/ar-2025-16
Preprint. Discussion started: 2 June 2025
© Author(s) 2025. CC BY 4.0 License.

2.3 On-line mass measurements with SHARP

The Synchronized Hybrid Ambient Real-time Particulate Monitor (SHARP, Thermo Scientific, Model 5030) is a real-time particulate monitor measuring at 1 s time resolution (Goohs et al., 2009). SHARP combines light scattering photometry and β–ray attenuation for continuous PM_{10} measurement. In SHARP the light scattering signal (nephelometer) is automatically calibrated against the beta attenuation mass sensor. The sample line inlet is placed on the roof of the cottage at 6 m height above the ground level and its flow rate is 16.7 lpm. The sample line is heated to reduce the humidity of the sample air. The temperature was fixed to 45 ˚C until August 2016 and to 35 ˚C after that. Sampling with SHARP at SMEAR II started in 2012.

2.4 Aerosol mass derived from the particle size distribution

The aerosol mass concentration for different size classes PM_{10}, $PM_{2.5}$ and PM_1 can also be estimated by combining the number size distributions measured with Differential Mobility Particle Sizer (DMPS) and Aerodynamic Particle Sizer (APS) and calculating the mass by assuming that the particles are spherical and have a constant density. The instrument set-ups for DMPS and APS are described in detail by Aalto et al. (2001). Briefly, the twin-DMPS consists of a long and a short Vienna type Differential Mobility Analyzers (DMA) and two condensation particle counters (CPC, TSI 3025 and TSI 3775). The DMPS inlet is placed on the roof of the hut at 8 m height and APS inlet at 5 m above ground level. The DMPS and APS systems provide aerosol number size distribution with a 10 min time resolution.

At SMEAR II, the DMPS measures the aerosol number size distribution in the electrical mobility equivalent diameter range of 3–1000 nm (Aalto et al., 2001). The APS (TSI 3320) measures the aerodynamic particle size distribution of particles with aerodynamic diameter within the range of 0.5–20 µm (Peters et al., 2006). To have comparable particle size distributions, we utilized the following conversion equation between the aerodynamic diameter (d_a) and the electrical mobility equivalent diameter (d_m):

$$\rho_0 d_a^2 = \rho_p d_m^2, \quad (1)$$

where ρ_p is the density of the particle and ρ_0 is the unit density of the particle (1 g cm^{-3}). The density of the particles is assumed to be 1.5 g cm^{-3} (Saarikoski et al., 2005). The mass of the particles measured with DMPS is calculated as:

https://doi.org/10.5194/ar-2025-16
Preprint. Discussion started: 2 June 2025
© Author(s) 2025. CC BY 4.0 License.

$$m_{\mathrm{DMPS}} = \frac{1}{6}\rho_{\mathrm{p}}\pi d_{\mathrm{m}}^3 \quad (2)$$

and the mass of the particles measured with APS:

$$m_{\mathrm{APS}} = \frac{1}{6}\rho_{\mathrm{p}}\pi d_{\mathrm{m}}^3 = \frac{1}{6}\rho_{\mathrm{p}}\pi\left[\left(\frac{\rho_0}{\rho_{\mathrm{p}}}\right)^{1/2} d_{\mathrm{a}}\right]^3 = \frac{1}{6}\pi\frac{\rho_0^{3/2}}{\rho_{\mathrm{p}}^{1/2}} d_{\mathrm{a}}^3. \quad (3)$$

The mass concentrations (PM_1, $PM_{2.5}$ and PM_{10}) were then calculated by integrating over the corresponding size range:

$$\mathrm{PM}_i = \int_{0\ \mu\mathrm{m}}^{0.6\ \mu\mathrm{m}} N_{\mathrm{DMPS}} \cdot m_{\mathrm{DMPS}} \mathrm{d}d_{\mathrm{m}} + \int_{0.6\ \mu\mathrm{m}}^{i\ \mu\mathrm{m}} N_{\mathrm{APS}} \cdot m_{\mathrm{APS}} \mathrm{d}d_{\mathrm{m}} \quad (4)$$

In practice, we utilized DMPS data from 0.003 to 0.6 µm and APS size distribution from 0.6 µm to 1 µm, 2.5 µm or 10 µm, depending on the mass fraction in question. Typical size distributions for different seasons are presented in Fig. 2.

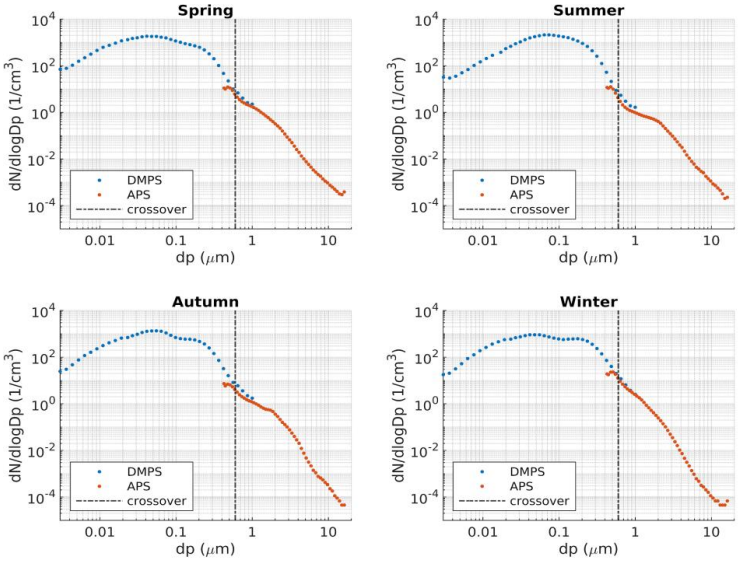

Figure 2: Seasonal median number size distributions for 2005–2020 at SMEAR II measured with a combination of DMPS and APS with a constant density assumption. The dash-dotted

https://doi.org/10.5194/ar-2025-16
Preprint. Discussion started: 2 June 2025
© Author(s) 2025. CC BY 4.0 License.

line indicates the crossover size between the instrument data to determine integrated mass concentrations.

2.5 Ancillary data

SO_2 and NO_x were measured at 16.8 m height above ground level at SMEAR II with gas analyzers by Thermo Fisher Scientific Inc., USA. SO_2 was measured with pulsed fluorescence technique, using model TEI 43CTL until September 2010 and model TEI 43i-TLE after that. NO_x concentration was measured with TEI 42CTL (molybdenum converter) until February 2007, then with TEI 42CTL (photolytic converter) until April 2011, and after that with TEI 42iTL (photolytic converter). Air mass origins were calculated using Hybrid Single-Particle Lagrangian Integrated Trajectory model (HYSPLIT) and divided to three sectors as described in Räty et al. (2023).

2.6 Correlations, bivariate fitting and long-term trend estimation

The Pearson's correlation coefficients between the mass concentrations from different instruments were calculated in Matlab, along with bivariate fitting (Cantrell, 2008). Before the analysis, we removed clear outliers that were further than 6 scaled median absolute deviations (MAD) away from the median using the Matlab built-in function *isoutlier*. The procedure was done for the whole dataset at once, i.e. without regarding for instance seasonal dynamics, but separately for each instrument and PM size. About 1.5 % of the data were removed. When comparing DMPS+APS and SHARP with the impactor data, we calculated 2–3 days' cumulative aerosol mass concentration to make DMPS+APS and SHARP measurements comparable to the impactor data time resolution.

The statistical significance of long-term trends in linear scale were calculated using the *mannkendall* function for Matlab (v1.1.0, 10.5281/zenodo.4495589). We applied the seasonal 3PW method, which utilizes three pre-whitening methods for the trend estimation (Hirsch et al., 1982). Pre-whitening methods by Kulkarni and von Stroch (1995) and Yue et al. (2002) remove lag-1 autocorrelation and autocorrelation on detrended data, enabling to determine the statistical significance of Mann-Kendall test reliably; of these the one with higher value is reported. Variance-corrected trend-free pre-whitening method by Wang et al. (2015) is used for calculation of Sen's slope, which leads to more accurate trend analysis (Collaud Coen et al., 2020).

https://doi.org/10.5194/ar-2025-16
Preprint. Discussion started: 2 June 2025
© Author(s) 2025. CC BY 4.0 License.

AEROSOL Research Discussions

3 Results and discussion

3.1 Comparison between the mass measurement methods

Here, we present the comparison between the different aerosol mass measurement techniques to validate our PM concentration data (Fig. 3 and S1). We found that the data from the different mass measurement techniques correlate well, with the correlation coefficients R>0.8 for all the measurements except between SHARP and impactor for which R=0.74 (Table 1). Thereby, the correlation was lower between the two direct mass measurements, SHARP and impactor, than between DMPS+APS derived and impactor or SHARP measurements, even though with the DMPS+APS method we had to assume constant density and spherical shape of the particles in the mass concentration calculations. In reality, the particle composition, density, and shape vary between different particles (Kannosto et al., 2008; Heikkinen et al., 2020), which could lead to the higher uncertainty in the indirect DMPS+APS mass calculations.

Table 1: Correlation coefficients between different PM measurement techniques. Correlation coefficient between SHARP and DMPS+APS in PM_{10} is 0.84. In all cases P-value << 0.05.

Method	Impactor, PM_{10}	Impactor, $PM_{2.5}$	Impactor, PM_1
DMPS+APS	0.84	0.86	0.88
SHARP	0.74	-	-

https://doi.org/10.5194/ar-2025-16
Preprint. Discussion started: 2 June 2025
© Author(s) 2025. CC BY 4.0 License.

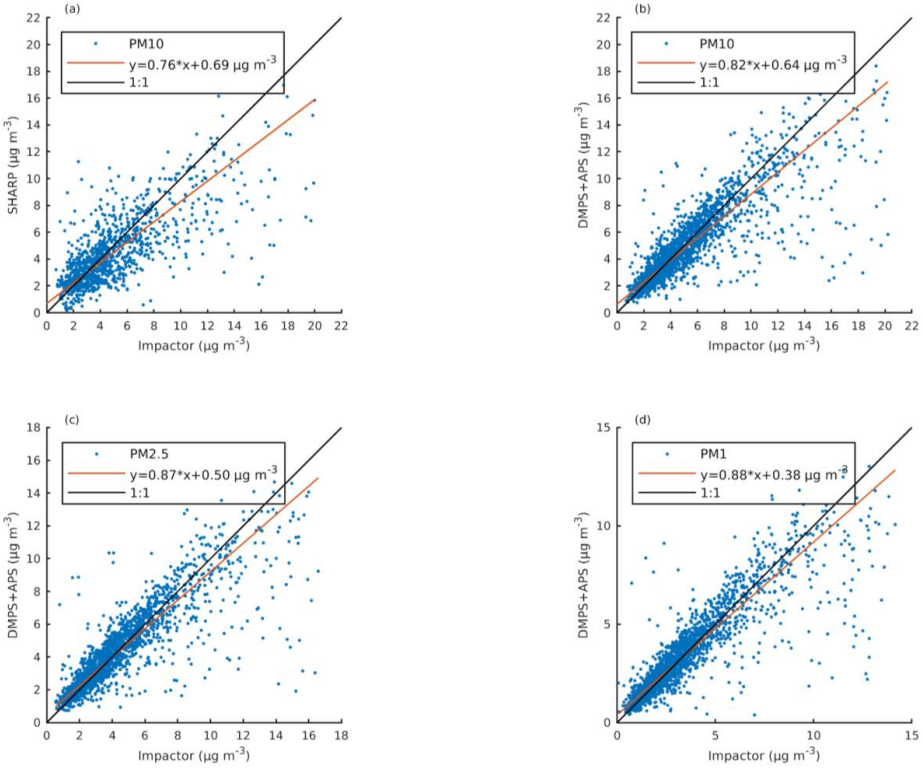

Figure 3: Correlation between the different mass measuring methods against impactor measurements a) PM_{10} from SHARP, b) PM_{10} from DMPS+APS, c) $PM_{2.5}$ from DMPS+APS, and d) PM_1 from DMPS+APS. Bivariate fit to the data is represented with a red line and 1:1 line is black. The data are averaged based on the impactor time resolution (2–3 days).

Comparing Fig. 3 and Fig. S1, it seems that the data points between SHARP and DMPS+APS are positioned more distinctly on the 1:1 line whereas the impactor data are scattered more towards higher concentrations in all size classes. After the inlet heating temperature reduction in SHARP from 45 to 35 °C, the PM_{10} values measured by SHARP were more comparable to those measured by impactor, except for the lowest and highest PM_{10} concentrations (Fig. S2). This indicates that the higher inlet heating temperature might have led to losses of semi-volatile compounds from the sample air of SHARP.

The measurement methods used in this study differ considerably from each other, and hence they are subject to different kinds of issues in PM monitoring. The impactor data, for example,

https://doi.org/10.5194/ar-2025-16
Preprint. Discussion started: 2 June 2025
© Author(s) 2025. CC BY 4.0 License.

is sensitive to any disturbances related to the weighing of the filters or evaporation of semi-volatile material from the filters during the long sampling time. Impactor is, however, the only purely weighing-based mass measurement at SMEAR II. Thus, in the next section, we compare all the other methods against the impactor data.

3.2 Seasonal variation and emission events

We explore the time series of PM concentrations to observe both the long-term trends and the differences between the seasons (Fig. 4 and S3). Mean values from 1991-2002 reported by Laakso et al. (2003) were also included in the figures to compare the results with the earlier values from SMEAR II. To enable the comparison with the values by Laakso et al. (2003), we divided our measurement period into shorter, approximately five-year periods (2005–2010, 2011–2015 and 2016–2020). The mean PM concentrations as well as median values are listed in Table 2.

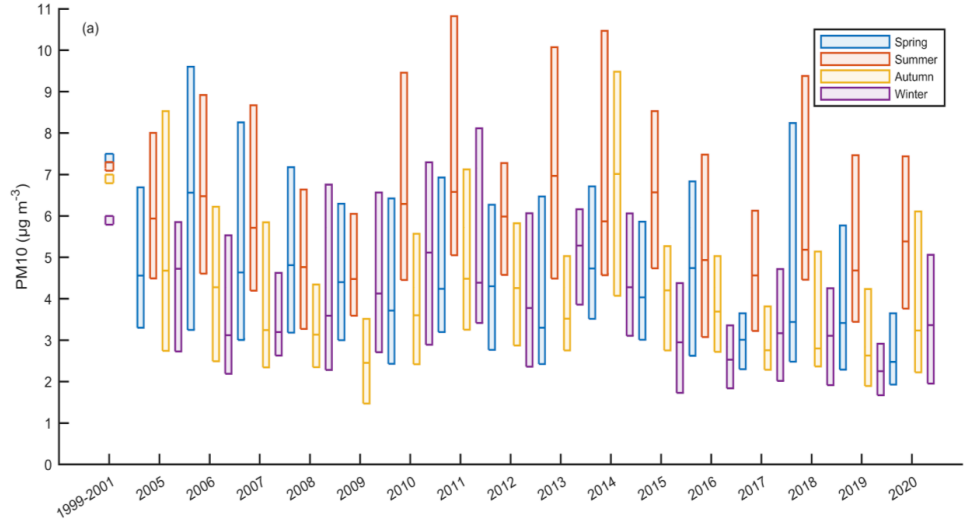

https://doi.org/10.5194/ar-2025-16
Preprint. Discussion started: 2 June 2025
© Author(s) 2025. CC BY 4.0 License.

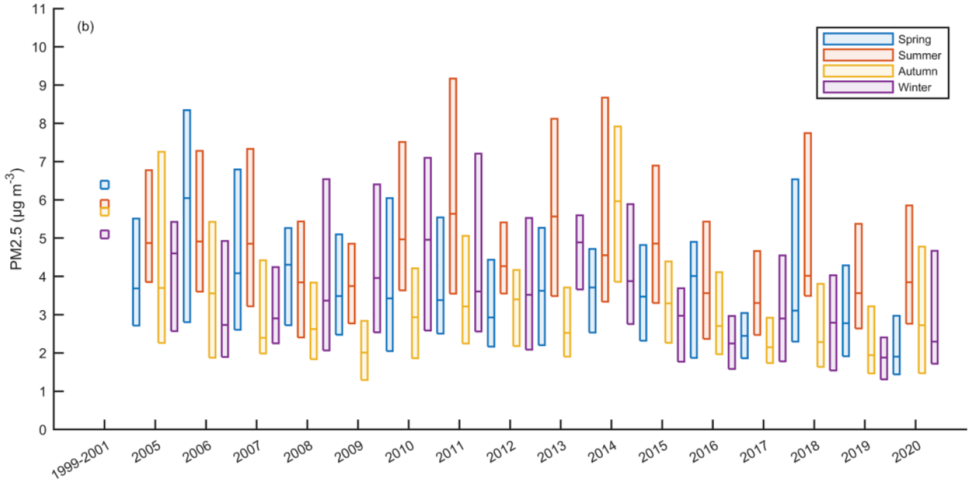

316

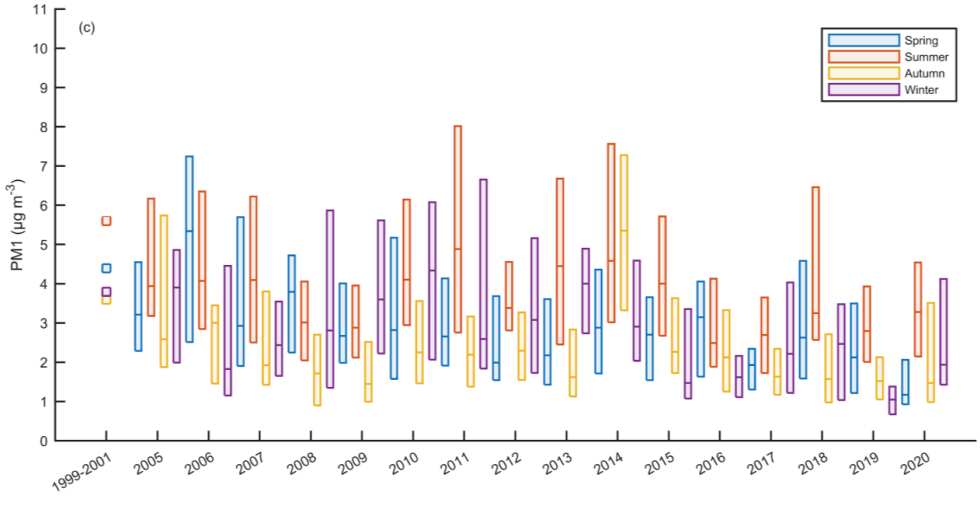

317

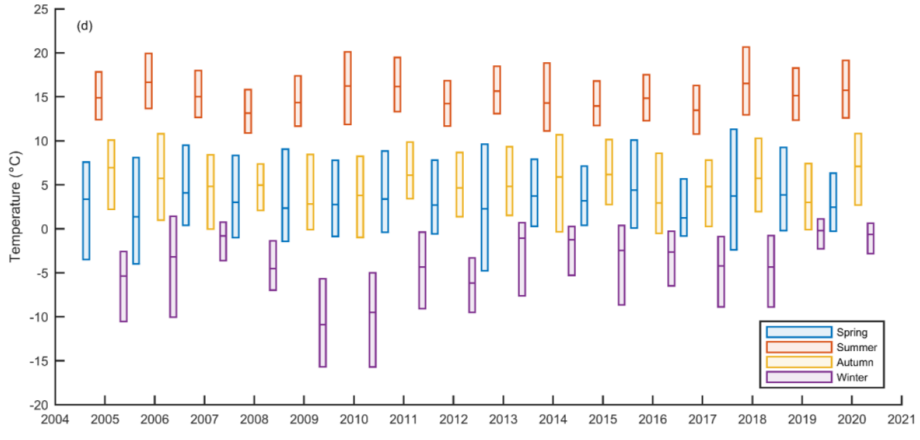

318

https://doi.org/10.5194/ar-2025-16
Preprint. Discussion started: 2 June 2025
© Author(s) 2025. CC BY 4.0 License.

AEROSOL Research Discussions

Figure 4: Seasonal median (a) PM_{10}, (b) $PM_{2.5}$ and (c) PM_1 concentrations measured with the impactor as well as (d) temperature and their 25 and 75 quartile ranges at SMEAR II. The tick mark is between summer and autumn of a year. Mean values for 1991–2002 are from Laakso et al. (2003).

Table 2: Average (mean / median) PM concentrations measured at SMEAR II. Values (mean) for 1999–2001 are from Laakso et al. (2003) and other values from this work. First number in each cell is the mean for the indicated period and following numbers are seasonal means. Unit is μg m^{-3}.

	1999–2001	2005–2010	2011–2015	2016–2020	2005–2020
PM_{10}, impactor	6.9	5.4 / 4.4	5.8 / 4.8	4.4 / 3.4	4.5 / 4.2
-Spring	7.4	5.9 / 4.7	5.3 / 4.2	4.4 / 3.3	4.2 / 4.1
-Summer	7.2	6.4 / 5.6	7.4 / 6.4	5.8 / 5.5	5.5 / 5.6
-Autumn	6.9	4.5 / 3.4	5.4 / 4.4	4.1 / 3.0	4.3 / 3.5
-Winter	5.9	4.7 / 3.9	5.0 / 4.4	3.3 / 2.8	3.9 / 3.6
PM_{10}, SHARP	-	-	4.2 / 3.6	4.7 / 4.0	5.2 / 3.8
-Spring			4.0 / 3.5	4.4 / 3.6	5.2 / 3.6
-Summer			4.9 / 4.4	6.0 / 5.5	6.5 / 5.1
-Autumn			3.8 / 3.1	4.7 / 3.8	4.7 / 3.7
-Winter			4.1 / 3.3	3.8 / 3.3	4.4 / 3.3
PM_{10},	-	5.5 / 4.8	4.8 / 4.0	4.2 / 3.4	4.9 / 4.1
DMPS+APS		5.8 / 4.9	4.4 / 3.9	4.1 / 3.5	4.8 / 4.1
-Spring		6.2 / 5.9	5.9 / 5.0	5.5 / 4.9	5.9 / 5.3
-Summer		4.8 / 3.9	4.2 / 3.3	3.8 / 2.8	4.3 / 3.4
-Autumn		5.5 / 4.7	4.7 / 3.9	3.5 / 2.9	4.7 / 3.9
-Winter					
$PM_{2.5}$, impactor	5.8	4.6 / 3.7	4.7 / 3.8	3.5 / 2.8	4.3 / 3.4
-Spring	6.4	5.0 / 4.1	4.2 / 3.5	3.4 / 2.6	4.2 / 3.3
-Summer	5.9	5.2 / 4.6	5.9 / 5.0	4.5 / 3.7	5.2 / 4.4
-Autumn	5.7	3.6 / 2.7	4.2 / 3.4	3.3 / 2.3	3.7 / 2.8
-Winter	5.1	4.4 / 3.5	4.5 / 3.8	2.9 / 2.4	4.0 / 3.2
$PM_{2.5}$,	-	4.7 / 4.0	4.1 / 3.4	3.6 / 3.0	4.2 / 3.6
DMPS+APS		4.8 / 4.2	3.7 / 3.2	3.4 / 2.9	4.1 / 3.4
-Spring		5.1 /4.8	4.9 / 4.2	4.6 / 4.2	4.9 / 4.5
-Summer		3.9 / 3.2	3.5 / 2.7	3.3 / 2.4	3.6 / 2.8
-Autumn		5.1 / 4.3	4.3 / 3.6	3.3 / 2.8	4.3 / 3.6
-Winter					
PM_1, impactor	4.3	3.8 / 3.0	3.8 / 2.9	2.7 / 2.1	3.4 / 2.7
-Spring	4.4	4.2 / 3.4	3.3 / 2.7	2.6 / 2.0	3.4 / 2.7
-Summer	5.6	4.4 / 3.7	4.9 / 4.0	3.5 / 3.0	4.2 / 3.5

https://doi.org/10.5194/ar-2025-16
Preprint. Discussion started: 2 June 2025
© Author(s) 2025. CC BY 4.0 License.

-Autumn	3.6	2.8 / 2.1	3.3 / 2.3	2.4 / 1.6	2.8 / 2.0
-Winter	3.8	3.7 / 2.8	3.7 / 3.0	2.3 / 1.7	3.3 / 2.5
PM_1,	-	3.8 / 3.3	3.3 / 2.6	3.0 / 2.4	3.4 / 2.8
DMPS+APS		3.9 / 3.3	2.9 / 2.5	2.8 / 2.3	3.3 / 2.6
-Spring		4.2 / 3.9	4.1 / 3.6	3.8 / 3.3	4.0 / 3.6
-Summer		3.0 / 2.3	2.7 / 1.9	2.6 / 1.8	2.8 / 2.1
-Autumn		4.3 / 3.4	3.5 / 2.8	2.7 / 2.0	3.5 / 2.8
-Winter					

The PM concentrations in all sizes have an overall decreasing trend during the measurement period, although there is a seasonal and interannual variation (Fig. 4 and S3). Additionally, the methods give slightly inconsistent results: DMPS+APS method shows constant decline in PM concentrations, whereas the impactor data shows slight increase in all PM sizes for 2011–2015 period for all seasons but spring (Table 2). SHARP data shows increased PM_{10} concentration between 2011–2015 and 2016–2020 for all other seasons except for winter, but this is likely explained by the decreased inlet heating temperature, changed between the two periods. Hence, no conclusion of the trend in SHARP data can be drawn. Despite the slight discrepancies between the methods, the PM mass concentrations are generally declining over the two decades of measurements. The trends are analyzed in more detail in the following section (Sect. 3.3).

The PM concentrations in all size classes are typically highest in summer and lowest in autumn (Table 2). In summertime, the surrounding boreal forest is a large source of organic compounds, which contribute to the aerosol load as shown already in several studies (e.g. Heikkinen et al., 2020, 2021; Yli-Juuti et al., 2021). Due to the temperature dependent activity of the forest, warm spells and heatwaves increase the VOC emissions, such as in 2018 (Neefjes et al., 2022), which is also evident in PM data in all size classes (Fig. 4). Additionally, pollen and other biological particles add up especially coarse mode particle mass at SMEAR II (Manninen et al., 2014).

Although PM mass concentrations are generally decreasing, certain events associated with higher PM levels, such as wildfires and volcanic eruptions, can be detected. In 2006 springtime as well as in 2006 and 2010 summer forest fires in eastern Europe increased the measured PM concentrations at SMEAR II (Fig. 4 and S3) (Leino et al., 2014). The growing seasons of 2006 and 2011 were exceptionally warm at SMEAR II based on the analysis spanning years 1996–2017 (Pysarenko et al., 2022), but the relatively high PM concentrations in spring 2010 and

https://doi.org/10.5194/ar-2025-16
Preprint. Discussion started: 2 June 2025
© Author(s) 2025. CC BY 4.0 License.

2011 can also be caused by the plume of ash and SO_2 from the erupted Eyjafjallajökull and Grímsvötn volcanoes in Iceland (Thomas et al., 2011; Gudmundsson et al., 2012; Tesche et al., 2012; Flanner et al., 2014). The mean PM concentrations in 2014 were affected by a six-month-long (from 31 August 2014 to 27 February 2015) eruption of the Bardarbunga volcano in Iceland, which Heikkinen et al. (2020) also noticed in the sulfate aerosol and SO_2 concentrations. During the eruptions, high concentrations of SO_2 and PM_{10} were measured over Europe (Cooke et al., 2011; Gislason et al., 2015; Ilyinskaya et al., 2017). The events are also associated with relatively high SO_2 and NO_x concentrations at SMEAR II (Fig. S4).

During the coldest winters 2009–2010 and 2010–2011, the measured PM concentrations were high. These years were also associated with high concentrations of SO_2 and NO_x (Fig. S4). Residential heating is known to be a source of particulate emissions as wood is burned for heating (Spindler et al., 2004; Viana et al., 2008; Barmpandimos et al., 2011). However, the coldest winter temperatures are typically measured in Finland when air is transported from the eastern continental areas (Sui et al., 2020). These, and particularly southeastern, areas are also a source of atmospheric pollutants (Riuttanen et al., 2013). Hence, rather than being local, the pollutants could also be advected to Finland. This is supported by the air mass source area analysis; the winters with higher fraction of easterly and European air masses had also higher PM levels (Fig. S5). Further, the measured concentrations are affected by the dynamics of the atmospheric boundary layer. Shallow boundary layer heights are measured during cold winter days, concentrating the anthropogenic pollutants close to the surface (Stull, 1988; Sinclair et al., 2022).

Overall, the air quality at SMEAR II was very good during our measurement period from 2005 to 2020 with mean values ranging from 3.4 µg m^{-3} for PM_1 measured by impactor to 5.2 µg m^{-3} for PM_{10} measured by SHARP. The values are in the same range as concentrations at European natural background sites reported in Van Dingenen et al. (2004). The lowest PM_{10} concentrations at Finnish urban sites measured between 1998 and 2003 were 9 µg m^{-3} while concentrations in Helsinki reached 20 µg m^{-3} (Anttila & Salmi, 2006). To give further perspective for the concentrations, in highly polluted areas in Beijing, China, the recorded PM_{10} values from 2004 to 2012, were 138 ± 93 µg m^{-3} for PM_{10}, 72 ±54 µg m^{-3} for $PM_{2.5}$ and 66 ± 56 µg m^{-3} for PM_1 (Liu et al., 2014).

https://doi.org/10.5194/ar-2025-16
Preprint. Discussion started: 2 June 2025
© Author(s) 2025. CC BY 4.0 License.

3.3 Long-term trends

Long-term trends are shown seasonally for each size class PM_{10}, $PM_{2.5}$ and PM_1 using impactor data (Fig. 5, S6, and S7). A decreasing trend is observed in each measured size class ranging from -0.012 to -0.064 µg m^{-3} y^{-1}. The largest decreases in all size classes are observed in spring and winter, whereas the decrease is the lowest in autumn. The decline is statistically significant at 95 % level in spring and winter, but not in summer and autumn. However, when calculating the trends from DMPS+APS data using 6–hour averages, the Mann-Kendall test revealed a statistically significant decrease in all size classes and seasons, ranging from -0.007 to -0.066 µg m^{-3} y^{-1} with similar seasonal distribution as with the impactor data (Table S1).

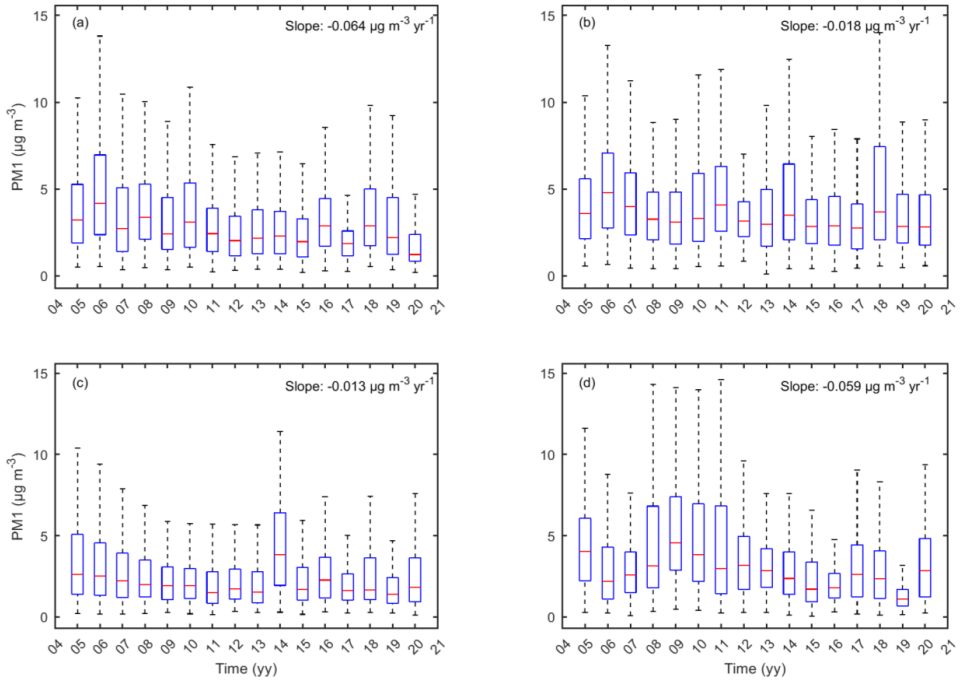

Figure 5: PM_1 concentration with the impactor method in (a) spring, (b) summer, (c) autumn, and (d) winter. Red horizontal line represents the median, the distance between the box edges shows the interquartile range, and whiskers extend to 1.5 times the interquartile range. Outliers are not shown. Slope represents trend calculated using seasonal Mann-Kendall test.

The seasonal differences in PM trends follow the trends observed also in SO_2 and NO_x concentrations (Fig. S8 and S9), indicating that the decrease in anthropogenic pollutants drive

https://doi.org/10.5194/ar-2025-16
Preprint. Discussion started: 2 June 2025
© Author(s) 2025. CC BY 4.0 License.

the decrease in PM concentrations. On the other hand, the lower summer and autumn time decline can also be explained by the high fraction (more than 50 %) of OA from the surrounding boreal forest in the PM mass concentration at SMEAR II (Heikkinen et al., 2020). Further, in Li et al. (2023) the concentrations of organic precursors have even been shown to have an increasing trend at SMEAR II.

In winter, biogenic OA precursors have minima in their concentrations (Heikkinen et al., 2020), and consequently the collected PM originates mostly from anthropogenic sources, such as traffic, industry, and different combustion processes (Forsberg et al., 2005; Anttila & Tuovinen, 2010). Moreover, many gaseous pollutants, emitted from anthropogenic processes and contributing to atmospheric chemistry or aerosol processes, have maxima in their seasonal cycle in spring and winter (Lyubovtseva et al., 2005; Anttila & Tuovinen, 2010; Riuttanen et al., 2013; Heikkinen et al., 2020), further affirming the contribution of anthropogenic pollution to the observed trends. Additionally, Banerji et al. (2025) showed that at SMEAR II, light absorbing aerosol peak in winter, being thus associated with e.g. black carbon from anthropogenic activities, while aerosol scattering peaks in summer and winter, being thus likely associated with organic aerosol in summer and sulfates in winter. They also found an increasing trend in single scattering albedo, indicating that the relative proportion of light absorbing aerosol decrease.

The seasonal difference in PM sources is visible also in the ratios between PM_1 to $PM_{2.5}$ and $PM_{2.5}$ to PM_{10} plotted against temperature bins (Fig. 6) as well as in monthly PM_1 to PM_{10} ratio (Fig. S10). The fraction of smaller particles increases in cold and warn temperatures, which could be attributed to rather local anthropogenic pollution during winters and SOA formation in summer (Fig. 6). In winters, nearly 80 % of PM_{10} consists actually of PM_1 (Fig. S10). The PM_1 to $PM_{2.5}$ and $PM_{2.5}$ to PM_{10} ratios exhibit small, but statistically significant at 95 % level, negative trends (Fig. S11), which could be attributed to the decline particularly in PM_1 concentration due to decreasing precursor concentrations.

https://doi.org/10.5194/ar-2025-16
Preprint. Discussion started: 2 June 2025
© Author(s) 2025. CC BY 4.0 License.

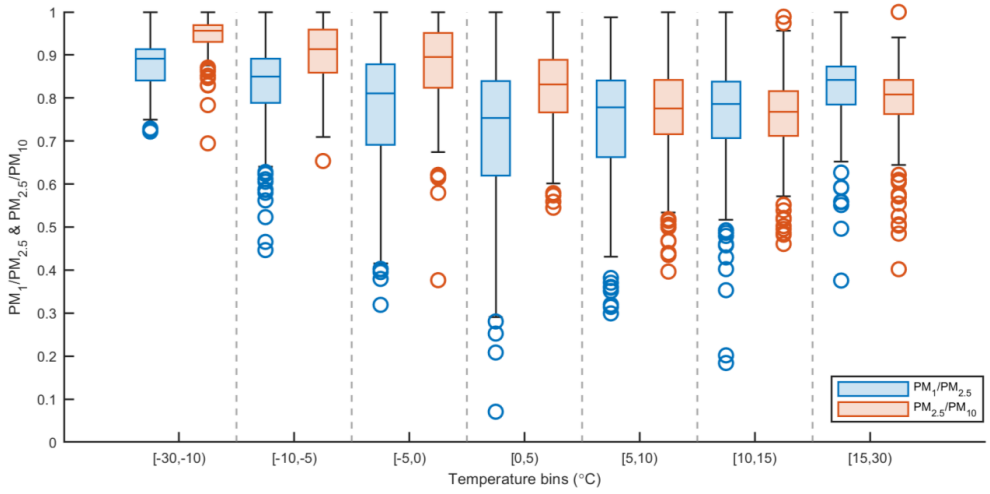

Figure 6: PM_1 to $PM_{2.5}$ and $PM_{2.5}$ to PM_{10} ratios in different temperature bins using impactor data. Horizontal line represents the median, the distance between the box edges shows the interquartile range, whiskers extend to 1.5 times the interquartile range, and data points even further from the median are presented with circles.

Generally, the PM concentrations have been observed to decrease in Europe (Spindler et al., 2004; Barmpadimos et al., 2011; Keuken et al., 2012; Guerreiro et al., 2014). However, in Guerreiro et al. (2014) small non-significant positive trends in PM_{10} and $PM_{2.5}$ were observed for Finnish rural background sites. In Anttila & Tuovinen (2010) both increasing and decreasing trends were detected, which was likely caused by the different measurement environments (urban, suburban, and industrial). Luoma et al. (2019) reported decreased light absorption of aerosol population at SMEAR II, indicating reduction in large particle concentration.

The connection between decreasing gaseous pollutant emissions and secondary aerosol concentrations has already been noted previously (e.g. Kyrö et al., 2014; Li et al., 2024) and decreasing PM trends in Europe have been connected to modernization of industry and heating systems as well as technology development of vehicles (Spindler et al., 2004; Barmpadimos et al., 2011; Keuken et al., 2012). Hence, the observed decrease in PM concentrations at SMEAR II can be connected to the emission reductions driven by air quality legislation.

https://doi.org/10.5194/ar-2025-16
Preprint. Discussion started: 2 June 2025
© Author(s) 2025. CC BY 4.0 License.

4 Conclusions

In this paper, different long-term aerosol mass concentration (PM_{10}, $PM_{2.5}$, PM_1) measurement techniques were compared and reported for the years 2005–2020 from SMEAR II, Finland. The direct mass concentration measurements with a cascade impactor and SHARP were compared with the mass concentrations calculated from the combined aerosol number size distributions of DMPS and APS. The results obtained using different methods are well comparable with the correlation coefficients of about 0.8.

The lower correlation values were connected to sampling methodologies: e.g., reducing the inlet heating temperature of SHARP, increased the correlation with the impactor. Additionally, although impactor measurements are simple and purely based on weighing of filters, the impactor data showed somewhat higher concentrations than the other two methods, which might stem from the difficulties related to weighing masses down to micrograms. Any disturbances or deposited dust particles can lead to overestimated mass concentration. This might even be the cause why impactor data showed statistically insignificant trends in summer and autumn while DMPS+APS data with similar absolute values resulted in statistically significant decreasing trend in PM concentration.

The measured masses were similar between all the methods, and hence we can conclude that all methods were applicable for long-term PM monitoring. Yet, we acknowledge that the comparison of PM concentrations measured with different techniques gives valuable information for data quality control purposes, as well as for validating the applicability of the different methods. Therefore, we encourage conducting extensive comparisons with different methods at each measurement site.

The PM concentrations at SMEAR II were generally low, mostly less than 5 μg m^{-3}, which clearly fell below the 20 μg m^{-3} limit by the EU air quality legislation. The highest PM concentrations at SMEAR II were measured in summer, when organic compounds from the surrounding boreal forest contribute to the measured PM mass. Peaks observed in the PM data can be related to transported particles from regions with e.g., forest fires or on-going volcanic eruptions.

https://doi.org/10.5194/ar-2025-16
Preprint. Discussion started: 2 June 2025
© Author(s) 2025. CC BY 4.0 License.

The measurements showed overall decreasing PM trends for all size classes and in all seasons, which can be attributed to the decrease in anthropogenic pollution due to legislation aiming for improved air quality. Importantly, the trends were weakest in summer when natural emissions of VOCs from the forest lead to the formation of OA. As these natural VOCs are projected to increase with increasing temperature, it is possible that summertime OA concentrations keep increasing in the future. Taken together with the declining anthropogenic emissions, the role of natural aerosol particles cloud be anticipated to signify in the future. Overall, the results emphasize the importance of the long-term measurements (Kulmala et al., 2023) for understanding atmospheric aerosol mass concentrations and factors controlling them. This is a requirement to quantify the relative roles of natural and anthropogenic sources to PM concentrations and ultimately to their impacts on health and climate.

Data availability

Aerosol data used in this study are available through EBAS database operated by NILU: https://ebas-data.nilu.no/ (accessed 05 May 2025), and temperature and trace gas data are published by Aalto et al. (2023) at https://doi.org/10.23729/23dd00b2-b9d7-467a-9cee-b4a122486039 (accessed: 05 May 2025). Air mass source area data is available upon request from the corresponding author.

Author contribution

The idea and design of the study were conceived by HMK, MK, and TP. IY wrote the manuscript, and together with LA analyzed the data and provided the visualizations. LH, TN, KL, EE, MK, and TP helped to interpret the results. IY, HMK, LA, PA, JA, JL, and JK were also providing measurement data. All authors also contributed in reviewing and commenting on the manuscript.

Competing interests

MK is member of the editorial board of Aerosol Research.

Acknowledgements

The authors acknowledge the SMEAR II and INAR RI infrastructure as well as ACTRIS for the data accessed from SmartSMEAR (https://smear.avaa.csc.fi/) and EBAS (https://ebas.nilu.no) databases. We thank also thank SMEAR II personnel and PIs for the long-term measurement data.

https://doi.org/10.5194/ar-2025-16
Preprint. Discussion started: 2 June 2025
© Author(s) 2025. CC BY 4.0 License.

Financial support

We acknowledge the following projects: ACCC Flagship funded by the Research Council of Finland grant number 337549 (UH), Academy professorship funded by the Research Council of Finland (grant no. 302958), Research Council of Finland projects no. 1325656, 311932, 334792, 316114, 325647, 325681, 347782, "Quantifying carbon sink, CarbonSink+ and their interaction with air quality" INAR project funded by Jane and Aatos Erkko Foundation, "Gigacity" project funded by Wihuri foundation, European Research Council (ERC) project ATM-GTP Contract No. 742206, European Union via Non-CO2 Forcers and their Climate, Weather, Air Quality and Health Impacts (FOCI) and Horizon 2020 research and innovation program under grant agreements No. 654109 and 739530 (ACTRIS).

References

Aalto, J., Aalto, P., Keronen, P., Kolari, P., Rantala, P., Taipale, R., Kajos, M., Patokoski, J., Rinne, J., Ruuskanen, T., Leskinen, M., Laakso, H., Levula, J., Pohja, T., Siivola, E., Kulmala, M., & Ylivinkka, I.: SMEAR II Hyytiälä forest meteorology, greenhouse gases, air quality and soil. University of Helsinki, Institute for Atmospheric and Earth System Research, 2023. https://doi.org/10.23729/23dd00b2-b9d7-467a-9cee-b4a122486039

Aalto, P., Hämeri, K., Becker, E., Weber, R., Salm, J., Mäkelä, J. M., Hoell, C., O'Dowd, C. D., Hansson, H.-C., Väkevä, M., Koponen, I. K., Buzorius, G., and Kulmala, M.: Physical characterization of aerosol particles during nucleation events, Tellus B: Chem. and Phys. Meteorol., 53, 344-358, 2001. DOI:10.1034/j.1600-0889.2001.d01-25.x

Anttila, P. and Salmi, T.: Characterizing temporal and spatial patterns of urban PM10 using six years of Finnish monitoring data. *Boreal Env. Res.* 11: 463–479, 2006.

Anttila, P. and Tuovinen J.-P.: Trends of primary and secondary pollutant concentrations in Finland in 1994–2007, *Atmospheric Environment*, 44, 30-41, 2010. doi:10.1016/j.atmosenv.2009.09.041

Banerji, S., Luoma, K., Ylivinkka, I., Ahonen, L., Kerminen, V.-M., and Petäjä, T.: Measurement Report: Optical properties of supermicron aerosol particles in a boreal environment, EGUsphere [preprint], https://doi.org/10.5194/egusphere-2025-1776, 2025.

https://doi.org/10.5194/ar-2025-16
Preprint. Discussion started: 2 June 2025
© Author(s) 2025. CC BY 4.0 License.

Barmpadimos, I., Hueglin, C., Keller, J., Henne, S., and Prévôt, A. S. H.: Influence of meteorology on PM10 trends and variability in Switzerland from 1991 to 2008, Atmos. Chem. Phys., 11, 1813-1835, 2011. DOI:10.5194/acp-11-1813-2011

Berner, A. and Luerzer, C. 1980. Mass size distributions of traffic aerosols at Vienna, J. Phys. Chem., 84, 2079-2083. DOI:10.1021/j100453a016

Chen, Y., Zang, L., Du, W., Xu, D., Shen, G., Zhang, Q., Zou, Q., Chen, J., Zhao, M., and Yao, D.: Ambient air pollution of particles and gas pollutants, and the predicted health risks from long-term exposure to PM(2.5) in Zhejiang province, China, Environ. Sci. Pollut. Res. Int., 25, 23833-23844, 2018. DOI:10.1007/s11356-018-2420-5

Cantrell, C. A.: Technical Note: Review of methods for linear least-squares fitting of data and application to atmospheric chemistry problems, Atmospheric Chemistry and Physics, 8(17), 5477–5487, 2008. DOI:10.5194/acpd-8-6409-2008

Collaud Coen, M., Andrews, E., Bigi, A., Martucci, G., Romanens, G., Vogt, F. P. A., and Vuilleumier, L.: Effects of the prewhitening method, the time granularity, and the time segmentation on the Mann–Kendall trend detection and the associated Sen's slope, Atmos. Meas. Tech., 13, 6945–6964, 2020. https://doi.org/10.5194/amt-13-6945-2020

Cooke, M.C., Francis, P.N., Millington, S., Saunders, R. and Witham, C.: Detection of the Grímsvötn 2011 volcanic eruption plumes using infrared satellite measurements. Atmos. Sci. Lett., 15: 321-327, 2011. https://doi.org/10.1002/asl2.506

Dusek, U., Frank, G. P., Hildebrandt, L., Curtius, J., Schneider, J., Walter, S., Chand, D., Drewnick, F., Hings, S., Jung, D., Borrmann, S., and Andreae, M. O.: Size Matters More Than Chemistry for Cloud-Nucleating Ability of Aerosol Particles, Science, 312, 1375-1378, 2006. DOI:10.1126/science.1125261

Flanner, M. G., A. S. Gardner,S. Eckhardt, A. Stohl, and J. Perket: Aerosol radiative forcing from the 2010 Eyjafjallajökull volcanic eruptions, J. Geophys. Res.Atmos., 119, 9481–9491, 2014. doi:10.1002/2014JD021977.

https://doi.org/10.5194/ar-2025-16
Preprint. Discussion started: 2 June 2025
© Author(s) 2025. CC BY 4.0 License.

584 Forsberg, B., Hansson, H.-C., Johansson, C., Areskoug, H., Söderlund, K., and Järvholm, B.:
585 Comparative Health Impact Assessment of Local and Regional Particulate Air Pollutants in
586 Scandinavia, Ambio, 34, 11-19, 2005. DOI:10.1639/0044-
587 7447(2005)034[0011:CHIAOL]2.0.CO;2
588
589 Gislason, S., Stefansdottir, G., Pfeffer, M. A., Barsotti, S., Jóhannsson, T., Galeczka, I., Bali,
590 E., Sigmarsson, O., Stefansson, A., Keller, N., Sigurdsson, A., Bergsson, B., Galle, B., Jacobo,
591 V. C., Arellano, S., Aiuppa, A., Jonasdottir, E., Eiriksdottir, E., Jakobsson, S., and
592 Gudmundsson, M.: Environmental pressure from the 2014–15 eruption of Bárðarbunga
593 volcano, Iceland, Geochem. Perspect. Lett., 1,84-93, 2015. DOI:10.7185/geochemlet.1509
594
595 Goohs, K., Lilienfeld, P., and Wilbertz, J.: A Synchronized Hybrid Real-Time Particulate
596 Monitor, EAC 2009 proceedings, 2009.
597
598 Gudmundsson, M., Thordarson, T., Höskuldsson, Á. et al. Ash generation and distribution
599 from the April-May 2010 eruption of Eyjafjallajökull, Iceland. Sci Rep 2, 572, 2012.
600 https://doi.org/10.1038/srep00572
601
602 Guenther, A. B., Zimmerman, P. R., Harley, P. C., Monson, R. K., and Fall, R.: Isoprene and
603 monoterpene emission rate variability: Model evaluations and sensitivity analyses, Journal of
604 Geophys. Res.: Atmos., 98, 12609-12617, 1993. DOI:10.1029/93JD00527
605
606 Guerreiro, C.B.B., Foltescu, V., and de Leeuw, F.: Air quality status and trends in Europe,
607 Atmospheric Environment, 98, 376-384, 2014.
608
609 Hari, P. and Kulmala, M.: Station for Measuring Ecosystem-Atmosphere Relations: (SMEAR
610 II), Boreal Environ. Res., 10, 315-322, 2005. DOI:10.1007/978-94-007-5603-8_9
611
612 Heikkinen, L., Äijälä, M., Riva, M., Luoma, K., Dällenbach, K., Aalto, J., Aalto, P., Aliaga,
613 D., Aurela, M., Keskinen, H., Makkonen, U., Rantala, P., Kulmala, M., Petäjä, T., Worsnop,
614 D., and Ehn, M.: Long-term sub-micrometer aerosol chemical composition in the boreal forest:
615 inter- and intra-annual variability, Atmos. Chem. Phys., 20, 3151-3180, 2020.
616 DOI:10.5194/acp-20-3151-2020
617

https://doi.org/10.5194/ar-2025-16
Preprint. Discussion started: 2 June 2025
© Author(s) 2025. CC BY 4.0 License.

618 Heikkinen, L., Äijälä, M., Daellenbach, K. R., Chen, G., Garmash, O., Aliaga, D., Graeffe, F.,
619 Räty, M., Luoma, K., Aalto, P., Kulmala, M., Petäjä, T., Worsnop, D., and Ehn, M.: Eight years
620 of sub-micrometre organic aerosol composition data from the boreal forest characterized using
621 a machine-learning approach, Atmos. Chem. Phys., 21, 10081–10109, 2021.
622 https://doi.org/10.5194/acp-21-10081-2021
623
624 Hirsch, R. M., Slack, J. R., and Smith, R. A.: Techniques of trend analysis for monthly water
625 quality data, Water Resour. Res., 18,107–121, 1982. DOI:10.1029/WR018i001p00107
626
627 Ilyinskaya, E., Schmidt, A., Mather, T. A., Pope, F. D., Witham, C., Baxter, P., Jóhannsson,
628 T., Pfeffer, M., Barsotti, S., Singh, A., Sanderson, P., Bergsson, B., McCormick Kilbride, B.,
629 Donovan, A., Peters, N., Oppenheimer, C., and Edmonds, M.: Understanding the
630 environmental impacts of large fissure eruptions: Aerosol and gas emissions from the 2014–
631 2015 Holuhraun eruption (Iceland), Earth Planet. Sci. Lett., 472, 309-322, 2017.
632 DOI:10.1016/j.epsl.2017.05.025
633
634 IPCC (2021). Climate Change 2021: The Physical Science Basis. Contribution of Working
635 Group I to the Sixth Assessment Report of the Intergovernmental Panel on Climate Change.
636 Cambridge University Press, Cambridge, United Kingdom and New York, NY, USA, 2021.
637
638 Isokääntä, S., Kim, P., Mikkonen, S., Kühn, T., Kokkola, H., Yli-Juuti, T., Heikkinen, L.,
639 Luoma, K., Petäjä, T., Kipling, Z., Partridge, D., and Virtanen, A.: The effect of clouds and
640 precipitation on the aerosol concentrations and composition in a boreal forest environment,
641 Atmos. Chem. Phys., 22, 11823–11843, https://doi.org/10.5194/acp-22-11823-2022, 2022.
642
643 Kannosto, J., Virtanen, A., Lemmetty, M., Mäkelä, J. M., Keskinen, J., Junninen, H., Hussein,
644 T., Aalto, P., and Kulmala, M.: Mode resolved density of atmospheric aerosol particles, Atmos.
645 Chem. Phys., 8, 5327-5337, 2008. DOI:10.5194/acp-8-5327-2008
646
647 Keskinen, H.-M., Ylivinkka, I., Heikkinen, L., Aalto, P. P., Nieminen, T., Lehtipalo, K., Aalto,
648 J., Levula, J., Kesti, J., Ahonen, L. R., Ezhova, E., Kulmala, M., and Petäjä, T.: Long-term
649 aerosol mass concentrations in southern Finland: instrument validation, seasonal variation and
650 trends, Atmos. Meas. Tech. Discuss. [preprint], 2020. https://doi.org/10.5194/amt-2020-447
651

https://doi.org/10.5194/ar-2025-16
Preprint. Discussion started: 2 June 2025
© Author(s) 2025. CC BY 4.0 License.

Keuken, M.P., Roemer, M.G.M., Zandveld, P., Verbeek, R.P., and Velders, G.J.M.: Trends in primary NO2 and exhaust PM emissions from road traffic for the period 2000-2020 and implications for air quality and health in the Netherlands, Atmospheric Environment, 54, 313-319, 2012.

Kulkarni, A., and von Storch, H.: Monte Carlo Experiments on the Effect of Serial Correlation on the Mann-Kendall Test of Trend Monte Carlo experiments on the effect, Meteorologische Zeitschrift, 82–85, 1995. DOI:10.1127/METZ/4/1992/82

Kulmala, M., Kontkanen, J., Junninen, H., Lehtipalo, K., Manninen, H. E., Nieminen, T., Petäjä, T., Sipilä, M., Schobesberger, S., Rantala, P., Franchin, A., Jokinen, T., Järvinen, E., Äijälä, M., Kangasluoma, J., Hakala, J., Aalto, P. P., Paasonen, P., Mikkilä, J., Vanhanen, J., Aalto, J., Hakola, H., Makkonen, U., Ruuskanen, T., Mauldin, R. L., Duplissy, J., Vehkamäki, H., Bäck, J., Kortelainen, A., Riipinen, I., Kurtén, T., Johnston, M. V., Smith, J. N., Ehn, M., Mentel, T. F., Lehtinen, K. E. J., Laaksonen, A., Kerminen, V.-M., and Worsnop, D. R.: Direct Observations of Atmospheric Aerosol Nucleation, Science, 339, 943-946, 2013. DOI: 10.1126/science.1227385

Kulmala, M., Lintunen, A., Lappalainen, H., Virtanen, A., Yan, C., Ezhova, E., Nieminen, T., Riipinen, I., Makkonen, R., Tamminen, J., Sundström, A.-M., Arola, A., Hansel, A., Lehtinen, K., Vesala, T., Petäjä, T., Bäck, J., Kokkonen, T., and Kerminen, V.-M.: Opinion: The strength of long-term comprehensive observations to meet multiple grand challenges in different environments and in the atmosphere, Atmos. Chem. Phys., 23, 14949–14971, 2023. https://doi.org/10.5194/acp-23-14949-2023

Kyrö, E.-M., Väänänen, R., Kerminen, V.-M., Virkkula, A., Petäjä, T., Asmi, A., Dal Maso, M., Nieminen, T., Juhola, S., Shcherbinin, A., Riipinen, I., Lehtipalo, K., Keronen, P., Aalto, P. P., Hari, P., and Kulmala, M.: Trends in new particle formation in eastern Lapland, Finland: effect of decreasing sulfur emissions from Kola Peninsula. Atmos. Chem. Phys., 14(9), 4383–4396, 2014.

Laakso, L., Hussein, T., Aarnio, P., Komppula, M., Hiltunen, V., Viisanen, Y., and Kulmala, M.: Diurnal and annual characteristics of particle mass and number concentrations in urban, rural and Arctic environments in Finland, Atmos. Environ., 37, 2629-2641, 2003.

https://doi.org/10.5194/ar-2025-16
Preprint. Discussion started: 2 June 2025
© Author(s) 2025. CC BY 4.0 License.

Laakso, L., Laakso, H., Aalto, P. P., Keronen, P., Petäjä, T., Nieminen, T., Pohja, T., Siivola, E., Kulmala, M., Kgabi, N., Molefe, M., Mabaso, D., Phalatse, D., Pienaar, K., and Kerminen, V. M.: Basic characteristics of atmospheric particles, trace gases and meteorology in a relatively clean Southern African Savannah environment, Atmos. Chem. Phys., 8, 4823-4839, 2008. DOI:10.1016/S1352-2310(03)00206-1

Laj, P., Lund Myhre, C., Riffault, V., Amiridis, V., Fuchs, H., Eleftheriadis, K., Petäjä, T., Salameh, T., Kivekäs, N., Juurola, E., Saponaro, G., Philippin, S., Cornacchia, C., Alados Arboledas, L., Baars, H., Claude, A., De Mazière, M., Dils, B., Dufresne, M., Evangeliou, N., Favez, O., Fiebig, M., Haeffelin, M., Herrmann, H., Höhler, K., Illmann, N., Kreuter, A., Ludewig, E., Marinou, E., Möhler, O., Mona, L., Eder Murberg, L., Nicolae, D., Novelli, A., O'Connor, E., Ohneiser, K., Petracca Altieri, R. M., Picquet-Varrault, B., van Pinxteren, D., Pospichal, B., Putaud, J., Reimann, S., Siomos, N., Stachlewska, I., Tillmann, R., Voudouri, K. A., Wandinger, U., Wiedensohler, A., Apituley, A., Comerón, A., Gysel-Beer, M., Mihalopoulos, N., Nikolova, N., Pietruczuk, A., Sauvage, S., Sciare, J., Skov, H., Svendby, T., Swietlicki, E., Tonev, D., Vaughan, G., Zdimal, V., Baltensperger, U., Doussin, J., Kulmala, M., Pappalardo, G., Sorvari Sundet, S., & Vana, M.: Aerosol, Clouds and Trace Gases Research Infrastructure (ACTRIS): The European Research Infrastructure Supporting Atmospheric Science. Bulletin of the American Meteorological Society, 105(7), E1098-E1136, 2024. https://doi.org/10.1175/BAMS-D-23-0064.1

Leino, K., Riuttanen, L., Nieminen, T., Dal Maso, M., Väänänen, R., Pohja, T., Keronen, P., Järvi, L., Aalto, P., Virkkula, A., Kerminen, V.-M., Petäjä, T., and Kulmala, M.: Biomass-burning smoke episodes in Finland from eastern European wildfires, Boreal Environ. Res., 19, 275-292, 2014. http://www.borenv.net/BER/pdfs/ber19/ber19B-275.pdf

Li X., Li H., Yao L., Stolzenburg D., Sarnela N., Vettikkat L., de Jonge R.W., Baalbaki R., Uusitalo H., Kontkanen J., Lehtipalo K., Daellenback K.R., Jokinen T., Aalto J., Keronen P., Schobesberger S., Nieminen T., Petäjä T., Kerminen V.-M., Bianchi F., Kulmala M., and Dada L.: Over 20 years of observations in the boreal forest reveal a decreasing trend of atmospheric new particle formation. *Boreal Env. Res*. 29: 25–52, 2024.

https://doi.org/10.5194/ar-2025-16
Preprint. Discussion started: 2 June 2025
© Author(s) 2025. CC BY 4.0 License.

719 Liu, Z., Hu, B., Wang, L, Wu, F., Gao, W., and Wang, Y.: Seasonal and diurnal variation in
720 particulate matter (PM_{10} and $PM_{2.5}$) at an urban site of Beijing: analyses from a 9-year study.
721 Environ. Sci. Pollut. Res. 22, 627–642, 2015. https://doi.org/10.1007/s11356-014-3347-0
722
723 Luoma, K., Virkkula, A., Aalto, P., Petäjä, T., and Kulmala, M.: Over a 10-year record of
724 aerosol optical properties at SMEAR II, Atmos. Chem. Phys., 19, 11363–11382, 2019.
725 https://doi.org/10.5194/acp-19-11363-2019
726
727 Lyubovtseva, Y. S., Sogacheva, L., Dal Maso, M., Bonn, B., Keronen, P. & Kulmala, M.:
728 Seasonal variations of trace gases, meteorological parameters, and formation of aerosols in
729 boreal forests. Boreal Env. Res. 10. 493–510, 2005.
730
731 Manavi, S.E.I., Aktypis, A., Siouti, E., Skyllakou, K., Myriokefalitakis, S., Kanakidou, M.,
732 Pandis, S.N. 2025. Atmospheric aerosol spatial variability: Impacts on air quality and climate
733 change. One Earth 8, 101237. https://doi.org/10.1016/j.oneear.2025.101237
734
735 Manninen, H., Bäck, J., Sihto-Nissilä, S.-L., Huffman, J., Pessi, A.-M., Hiltunen, V., Aalto, P.
736 P., Hidalgo, P., Hari, P., Saarto, A., Kulmala, M. and Petäjä, T.: Patterns in airborne pollen and
737 other primary biological aerosol particles (PBAP), and their contribution to aerosol mass and
738 number in a boreal forest, Boreal Env. Res., 19 (suppl. B), 383-405, 2014.
739
740 Makkonen, U., Virkkula, A., Hellén, H., Hemmilä, M., Sund, J., Äijälä, M., Ehn, M., Junninen,
741 H., Keronen, P., Petäjä, T., Worsnop, D. R., Kulmala, M., and Hakola, H.: Semi-continuous
742 gas and inorganic aerosol measurements at a boreal forest site: seasonal and diurnal cycles of
743 NH3, HONO and HNO3, Boreal Env. Res., 19 (suppl. B), 311-328, 2014.
744
745 Maynard, A. D., and Kuempel, E. D. Airborne Nanostructured Particles and Occupational
746 Health. J Nanopart Res 7, 587–614, 2005. https://doi.org/10.1007/s11051-005-6770-9
747
748 Neefjes I., Laapas M., Liu Y., Médus E., Miettunen E., Ahonen L., Quéléver L., Aalto J., Bäck
749 J., Kerminen V-M., Lamplahti J., Luoma K., Mäki M., Mammarella I., Petäjä T., Räty M.,
750 Sarnela N., Ylivinkka I., Hakala S., Kulmala M., Nieminen T. & Lintunen A.: 25 years of
751 atmospheric and ecosystem measurements in a boreal forest — Seasonal variation and
752 responses to warm and dry years, Boreal Env. Res. 27: 1–31, 2022.

https://doi.org/10.5194/ar-2025-16
Preprint. Discussion started: 2 June 2025
© Author(s) 2025. CC BY 4.0 License.

Nenes, A., Pandis, S. N., Weber, R. J., and Russell, A.: Aerosol pH and liquid water content determine when particulate matter is sensitive to ammonia and nitrate availability, Atmos. Chem. Phys., 20, 3249–3258, 2020. https://doi.org/10.5194/acp-20-3249-2020

Neusüß, C., Weise, D., Birmili, W., Wex, H., Wiedensohler, A., and Covert, D. S.: Size-segregated chemical, gravimetric and number distribution-derived mass closure of the aerosol in Sagres, Portugal during ACE-2, Tellus B: Chem. Phys. Meteorol., 52, 169-184, 2000. DOI:10.1034/j.1600-0889.2000.00039.x

Olenius, T., Yli-Juuti, T., Elm, J., Kontkanen, J., and Riipinen, I.: New Particle Formation and Growth: Creating a New Atmospheric Phase Interface. In Faust, J. A. and House, J. E., editors, Physical Chemistry of Gas-Liquid Interfaces, Developments in Physical & Theoretical Chemistry, pages 315–352. Elsevier, 2018.

Occhipinti, L. G., and Oluwasanya, P. W.: Particulate Matter Monitoring: Past, Present and Future. Int J Earth Environ Sci 2: 144, 2017. doi: https://doi.org/10.15344/2456-351X/2017/144

Peters, T., Ott, D., and O'Shaughnessy, P.: Comparison of the GRIMM 1.108 and 1.109 Portable Aerosol Spectrometer to the TSI 3321 Aerodynamic Particle Sizer for Dry Particles, Ann. Occup. Hyg., 50, 843-850, 2006. DOI:10.1093/annhyg/mel067

Pope, C., Burnett, R. T., and Thun, M. J.: Lung cancer, cardiopulmonary mortality, and long-term exposure to fine particulate air pollution, J. Amer. Med. Assoc., 287, 1132-1141, 2003. doi: 10.1001/jama.287.9.1132

Pysarenko, L., Krakovska, S., Savenets, M., Ezhova, E., Lintunen, A., Petäjä, T., Bäck, J. and Kulmala, M.: Two-decade variability of climatic factors and its effect on the link between photosynthesis and meteorological parameters: example of Finland's boreal forest, Boreal Environment Research, 27, 131-144, 2022.

https://doi.org/10.5194/ar-2025-16
Preprint. Discussion started: 2 June 2025
© Author(s) 2025. CC BY 4.0 License.

Pöschl, U.: Atmospheric Aerosols: Composition, Transformation, Climate and Health Effects. Angewandte Chemie International Edition, 44: 7520-7540, 2005. https://doi.org/10.1002/anie.200501122

Riipinen, I., Yli-Juuti, T., Pierce, J. R., Petäjä, T., Worsnop, D. R., Kulmala, M., and Donahue, N. M.: The contribution of organics to atmospheric nanoparticle growth. Nature Geoscience, 5(7):453–458, 2012.

Rinne, J., Ruuskanen, T., Reissell, A., Taipale, R., Hakola, H., and Kulmala, M.: On-line PTR-MS measurements of atmospheric concentrations of volatile organic compounds in a European boreal forest ecosystem, Boreal Environ. Res., 10, 425-436, 2005. http://www.borenv.net/BER/archive/pdfs/ber10/ber10-425.pdf

Riuttanen, L., Hulkkonen, M., Dal Maso, M., Junninen, H., and Kulmala, M.: Trajectory analysis of atmospheric transport of fine particles, SO_2, NO_x and O_3 to the SMEAR II station in Finland in 1996–2008, Atmos. Chem. Phys., 13, 2153–2164, 2013. https://doi.org/10.5194/acp-13-2153-2013

Saarikoski, S., Mäkelä, T., Hillamo, R., Aalto, P., Kerminen, V.-M., and Kulmala, M.: Physicochemical characterization and mass closure of size-segregated atmospheric aerosols in Hyytiälä, Finland, Boreal Environ. Res., 10, 386-400, 2005.

Schraufnagel, D.E.: The health effects of ultrafine particles. Exp. Mol. Med. 52, 311–317, 2020. https://doi.org/10.1038/s12276-020-0403-3

Seinfeld, J. and Pandis, S.: *Atmospheric chemistry and physics: from air pollution to climate change.* Second edition. John Wiley & Sons, New Jersey, USA, 2006.

Shiraiwa, M., Ueda, K, Pozzer, A., Lammel, G., Kampf, C. J., Fushimi, A., Enami, S., Arangio, A. M., Fröhlich-Nowoisky, J., Fujitani, Y., Furuyama, A., Lakey, P. S. J., Lelieveld, J., Lucas, K., Morino, Y., Pöschl, U., Takahama, S., Takami, A., Tong, H., Weber, B., Yoshino, A., and Sato, K.: Aerosol Health Effects from Molecular to Global Scales, Environmental Science & Technology, 51 (23), 13545-13567, 2017.
DOI: 10.1021/acs.est.7b04417

https://doi.org/10.5194/ar-2025-16
Preprint. Discussion started: 2 June 2025
© Author(s) 2025. CC BY 4.0 License.

Shukla, K., and Aggarwal, S.G.: A Technical Overview on Beta-Attenuation Method for the Monitoring of Particulate Matter in Ambient Air. Aerosol Air Qual. Res. 22, 220195, 2022. https://doi.org/10.4209/aaqr.220195

Sinclair, V. A., Ritvanen, J., Urbancic, G., Statnaia, I., Batrak, Y., Moisseev, D., and Kurppa, M.: Boundary-layer height and surface stability at Hyytiälä, Finland, in ERA5 and observations, Atmos. Meas. Tech., 15, 3075–3103, 2022. https://doi.org/10.5194/amt-15-3075-2022

Spindler, G., Müller, K., Brüggemann, E., Gnauk, T., and Herrmann, H.: Long-term size-segregated characterization of PM10, PM2.5, and PM1 at the IfT research station Melpitz downwind of Leipzig (Germany) using high and low-volume filter samplers, Atmos. Environ., 38, 5333-5347, 2004. DOI:10.1016/j.atmosenv.2003.12.047

Stull, R. B. 1988. *An Introduction to Boundary Layer Meteorology*, Springer Dordrecht.

Sui, C., Yu, L., and Vihma, T.: Occurrence and drivers of wintertime temperature extremes in Northern Europe during 1979–2016. *Tellus A: Dynamic Meteorology and Oceanography*, *72*(1), 1–19., 2020. https://doi.org/10.1080/16000870.2020.1788368

Tesche, M., P. Glantz, C. Johansson, M. Norman, A. Hiebsch, A. Ansmann, D. Althausen, R. Engelmann, and Seifert, P.: Volcanic ash over Scandinavia originating from the Grímsvötn eruptions in May 2011, *J. Geophys. Res.*, 117, D09201, 2012. doi:10.1029/2011JD017090

Thomas, H. E. and Prata, A. J.: Sulphur dioxide as a volcanic ash proxy during the April–May 2010 eruption of Eyjafjallajökull Volcano, Iceland, Atmos. Chem. Phys., 11, 6871–6880, 2011. https://doi.org/10.5194/acp-11-6871-2011

Van Dingenen, R., Raes, F., Putaud, J.-P., Baltensperger, U., Charron, A., Facchini, M., Decesari, S., Sandro, F., Gehrig, R., Hansson, H.-C., Harrison, R., Hüglin, C., Jones, A., Laj, P., Lorbeer, G., Maenhaut, W., Palmgren, F., Querol, X., Rodriguez, S., and Wåhlin, P.: A European aerosol phenomenology - 1: Physical characteristics of particulate matter at kerbside,

https://doi.org/10.5194/ar-2025-16
Preprint. Discussion started: 2 June 2025
© Author(s) 2025. CC BY 4.0 License.

urban, rural and background sites in Europe, Atmos. Environ., 38, 2561-2577, 2004. DOI:10.1016/j.atmosenv.2004.01.040

Viana, M., Kuhlbusch, T.A.J., Querol, X., Alastuey, A., Harrison, R.M., Hopke, P.K., Winiwarter, W., Vallius, M., Szidat, S., Prévôt, A.S.H., Hueglin, C., Bloemen, H., Wåhlin, P., Vecchi, R., Miranda, A.I., Kasper-Giebl, A., Maenhaut, W., and Hitzenberger, R.: Source apportionment of particulate matter in Europe: A review of methods and results, Journal of Aerosol Science, 39: 10, 827-849, 2008. https://doi.org/10.1016/j.jaerosci.2008.05.007.

Wang, W., Chen, Y., Becker, S., and Liu, B.: Linear trend detection in serially dependent hydrometeorological data based on a variance correction Spearman rho method, Water, 7(12), 7045–7065, 2015. DOI:10.3390/w7126673

Wang, J., Xing, J., Mathur, R., Pleim, J. E., Wang, S., Hogrefe, C., Gan, J.-M., Wong, D. C., and Hao, J.: Historical Trends in $PM_{2.5}$-Related Premature Mortality during 1990–2010 across the Northern Hemisphere,
Environmental Health Perspectives 125:3, 2017. https://doi.org/10.1289/EHP298

WHO global air quality guidelines. Particulate matter (PM2.5 and PM10), ozone, nitrogen dioxide, sulfur dioxide and carbon monoxide. Geneva: World Health Organization, 2021.

Yli-Juuti, T., Mielonen, T., Heikkinen, L., Arola, A., Ehn, M., Isokääntä, S., Keskinen, H.-M., Kulmala, M., Laakso, A., Lipponen, A., Luoma, K., Mikkonen, S., Nieminen, T., Paasonen, P., Petäjä, T., Romakkaniemi, S., Tonttila, J., Kokkola, H., and Virtanen, A.: Significance of the organic aerosol driven climate feedback in the boreal area. Nature Communications, 12(1):1–9, 2021.

Yue, S., Pilon, P., Phinney, B., and Cavadias, G.: The influence of autocorrelation on the ability to detect trend in hydrological series, Hydrol. Process., 16(9), 1807–1829, 2002. https://doi.org/10.1002/hyp.1095